

Cite this: *Lab Chip*, 2012, 12, 3221–3234

www.rsc.org/loc

Acoustofluidics 18: Microscopy for acoustofluidic micro-devices

Martin Wiklund, Hjalmar Brismar and Björn Önfelt

DOI: 10.1039/c2lc40757d

In this tutorial review in the thematic series “Acoustofluidics”, we discuss the implementation and practice of optical microscopy in acoustofluidic micro-devices. Examples are given from imaging of acoustophoretic manipulation of particles and cells in microfluidic channels, but most of the discussion is applicable to imaging in any lab-on-a-chip device. The discussion includes basic principles of optical microscopy, different microscopy modes and applications, and design criteria for micro-devices compatible with basic, as well as advanced, optical microscopy.

last three years. If we include the keyword “imaging”, the number increases to 70%. The described work in these publications range from basic visual inspection of microchannels using a standard microscope (e.g., in acoustophoresis¹ and dielectrophoresis²), to advanced optical imaging,^{3–5} and imaging methods integrated within the micro-device itself.^{6–8} Even if it is obvious that many researchers in the microfluidic field routinely use microscopy, it is clear that the specific requirements high quality microscopy can pose on the device design are not always a top priority.

In this tutorial review we focus on the use and implementation of microscopy for lab-on-a-chip devices, with special emphasis on micro-devices for ultrasonic manipulation of cells. The review includes the basic principles and practice of microscopy (Section II), a brief overview of different modes of microscopy (Section III), and finally some practical guidelines and recommendations to consider when using microscopy for studies in a micro-device along with examples of such implementations in studies of acoustofluidic micro-devices (Section IV).

The first question to ask when identifying the microscope to use is: What is the size of the object of interest and how

finely do details need to be resolved in the images? Typical objects studied with optical microscopy range from a few millimeters all the way down to the resolution limit, approximately 200 nm in optical microscopy (Fig. 1). The resolution required in an experiment will define which type of microscope to use. Often one must make a compromise between resolution and ease of use. High resolution comes with short working distance and short depth of field, factors that should already have been considered when designing the micro-device. The resolution limit of the selected microscope and its lenses is defined by the natural law of diffraction, discussed in more detail in Section II B.

The second question to ask is: How do I get contrast between the imaged object and its background/surroundings? This question is particularly important when imaging cells. A biological cell suspended in water is a highly transparent, weakly refracting object which may appear invisible unless a contrast-enhancing method such as phase contrast, dark field, differential interference contrast (DIC) or fluorescence is used. The different contrast-enhancing methods are described in more detail in Sect III, with examples shown in Section IV.

I. Introduction

One of the most frequently used tools for investigation of a lab-on-a-chip devices is the optical microscope. For example, about half of all papers published in *Lab on a Chip* over the last decade contained the keyword “microscope” or “microscopy”, with an increasing trend over the

Department of Applied Physics, Royal Institute of Technology, Stockholm, SE-10691, Sweden.
E-mail: martin@bio.x.kth.se;
Tel: +46 8 5537 8134

Foreword

Finding out what is actually happening with the cells and particles inside a microfluidic device is of paramount importance in order to evaluate function or performance, and acoustofluidic devices are no exception. Visual inspection with microscopy is therefore a common and useful tool. In the eighteenth paper of 23 in the *Lab on a Chip* tutorial series on Acoustofluidics, Martin Wiklund, Hjalmar Brismar and Björn Önfelt describe the basic principles of optical microscopy and different modes of microscopy. Different aspects of implementation of optical microscopy with an acoustofluidic micro-device as well as some practical advice regarding implementation of such systems with lab-on-a-chip devices are also given.

Andreas Lenshof – coordinator of the Acoustofluidics series

II. Basic principles of optical microscopy

Generally, optical microscopy is classified as either wide-field microscopy or different variations of point-illumination/detection techniques, e.g. confocal microscopy. We will start by discussing wide-field microscopy, which is similar to standard optical microscopy as the entire field of view is uniformly illuminated with light and the image is observed by

the operator through the eyepiece or by a camera.

A schematic illustration is shown in Fig. 2. The main parts of the microscope can be divided into: (1) the illumination system (either epi- and/or trans-illumination), (2) the objective, (3) optional filters, and (4) the imaging detector (either an eye-piece and the eye, or a camera). The most basic implementation of a microscope has only an objective and imaging detector; while more

advanced microscopes also have an integrated illumination system. A filter cube is typically used in fluorescence microscopy for separation of fluorescence from the excitation light. It is important to keep in mind that the objective is the single most important component of the microscope. Often only the manufacturer and model of the microscope is specified in scientific papers using microscope images. Unless the objective used is specified, this information is of limited value. Finally, Fig. 3 shows how the different optical components are assembled in practice for both an upright (looking from above) and inverted microscope (looking from below). The upright microscope corresponds to the schematic arrangement in Fig. 2, while the inverted microscope corresponds to flipping Fig. 2 vertically.

II A. Illumination system

We can start by looking at the trans-illumination, wide-field microscope with a “human detector” (right part of Fig. 2) by following the light rays from the light source via the specimen (object) and into the detector where the magnified image of the object should be located. Naturally, most specimens of interest are not inherently luminous and, therefore, need to be



Martin Wiklund

Martin Wiklund is Associate Professor in applied physics at the Dept. of Applied Physics, Royal Institute of Technology (KTH), Stockholm, Sweden. He received his M.Sc. in engineering physics from Lund University in 1999 and his Ph.D. in physics from the Dept. of Physics, KTH, Stockholm, in 2004. In 2004–2005, he was postdoctoral fellow at the Fraunhofer Institute for Biomedical Engineering (IBMT), Berlin, Germany. He returned to KTH in 2005, becoming an Assistant Professor in 2006, and Associate Professor in 2009. Currently, Wiklund's research is focused on acoustic and optical methods for micro-scaled handling and characterization of cells, and applications of the methods to biomedical research. He is also a lecturer in various courses in basic physics, optics, ultrasound physics and diagnostic ultrasound. He is author to >25

peer-reviewed journal papers, >50 conference contributions, including >20 invited talks; two patents and a recent book chapter (“Ultrasonic Manipulation of Single Cells”, In: Single-Cell Analysis: Methods and Protocols, Methods in Molecular Biology, vol. 853, Springer, 2012).



Hjalmar Brismar

Hjalmar Brismar is Professor of Biological Physics at the Dept. of Applied Physics, Royal Institute of Technology (KTH) and at the Dept. of Women's and Children's Health, Karolinska Institutet (KI), Stockholm, Sweden. He is also director of BioImaging at the national research center, Science for Life Laboratory in Stockholm. He received a M.Sc. Engineering Physics in 1991 and a Ph.D. in Physics in 1995, both at KTH. During 1995–96 he did postdoc training in the Biomedical

Imaging laboratory at Harvard School of Public Health, Harvard University, Boston. In 1997 he became Assistant Professor and was promoted in 2002 to Associate Professor in experimental pediatrics at KI. In 2003 he was recruited to KTH as full professor and chair of the division of Cell Physics. Brismar's research concerns cellular biophysics and microscopy in general and the spatio-temporal regulation of membrane proteins in neuronal synapses in particular.



Björn Önfelt

Björn Önfelt is an Associate Professor at the Dept. of Applied Physics, Royal Institute of Technology (KTH) and the Dept. of Microbiology, Tumor and Cell Biology, Karolinska Institutet (KI), Stockholm, Sweden. He received a M.Sc. in chemistry at Gothenburg University in 1997, and a Ph.D. in physical chemistry at Chalmers University of Technology, Gothenburg in 2002. During 2003–2006 he did a postdoc at the division of Cell and Molecular Biology and the

Dept. of Physics at Imperial College London, UK. In 2007 he became an Assistant Professor at KI and KTH funded by the Swedish Research Council. In 2008 he was selected as a Future Research Leader by the Swedish Foundation for Strategic Research. He was promoted to Associate Professor at KTH in 2012. Önfelt's research is focused on approaches combining microfabrication and live cell imaging to characterize the interaction between natural killer cells or T-cells and target cells, integrating basic science with applications in stem cell transplantation and cell therapy.

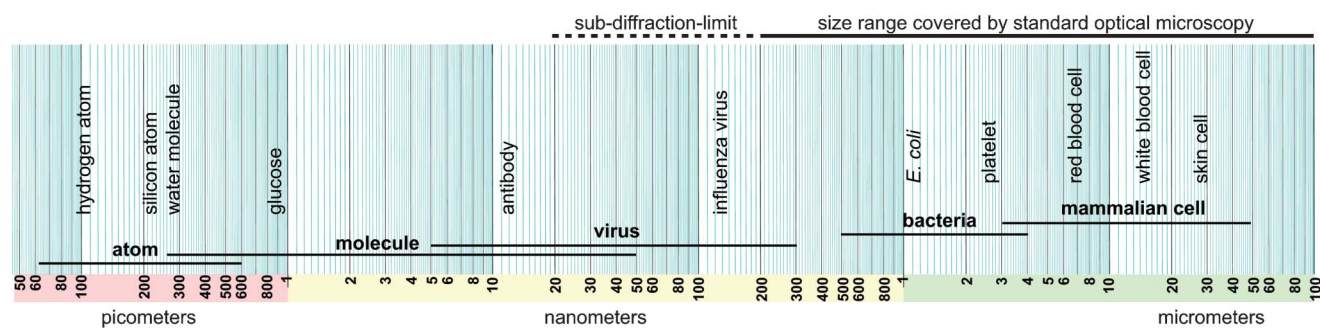


Fig. 1 Schematic diagram of relative sizes of different biological objects of interest and the coverage of optical microscopy operating in the visible light regime.

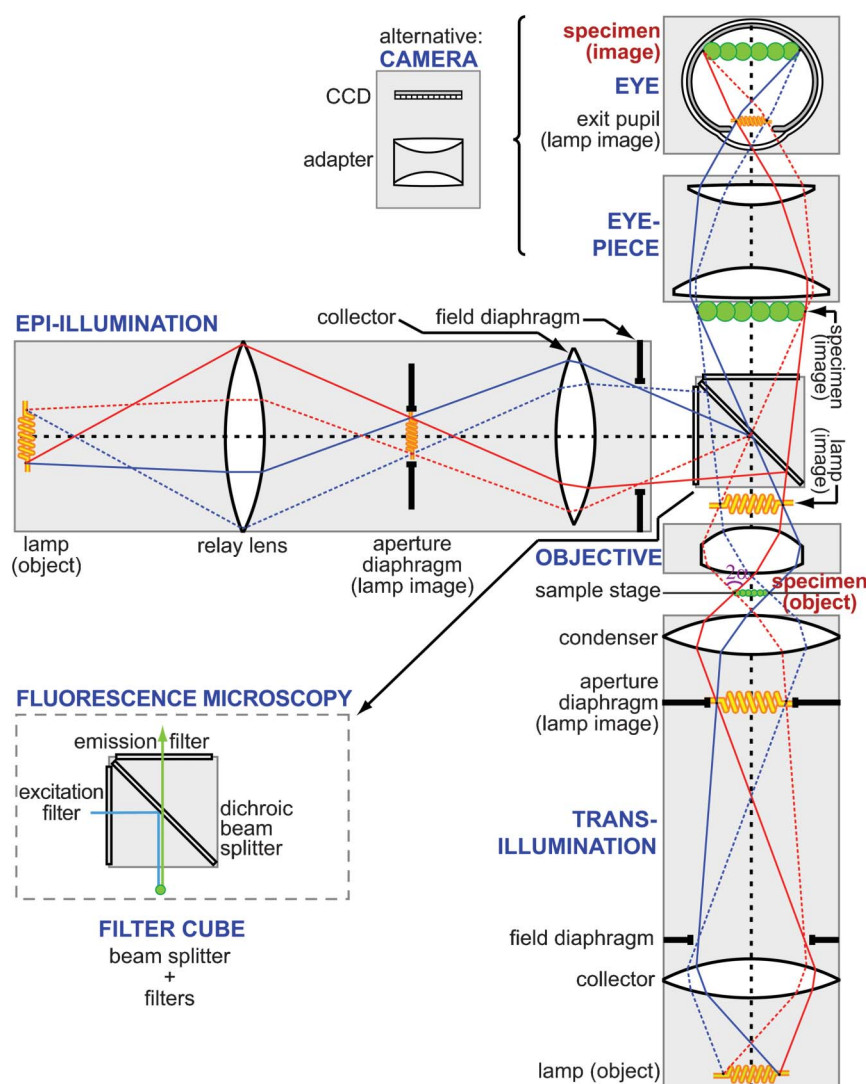


Fig. 2 Schematic of a wide-field optical microscope including an illustration of light rays from the light source to the detector. The diagram illustrates trans-illumination bright-field microscopy, epi-illumination bright-field microscopy and epi-fluorescence microscopy. The difference between epi-illumination bright-field and epi-fluorescence microscopy is the choice of filter cube/beam splitter: In the former, a simple semi-transparent mirror is sufficient, while in the latter, the beam splitter is wavelength-sensitive (short wavelengths are reflected while long wavelengths are transmitted). The light rays illustrate the Köhler illumination technique, which is the standard method of uniform illumination of the specimen. Finally, the two standard detection options in wide-field microscopy are illustrated: Manual observation through an eyepiece, or electronic detection with a camera. The figure is based on illustrations from Ref. 12.

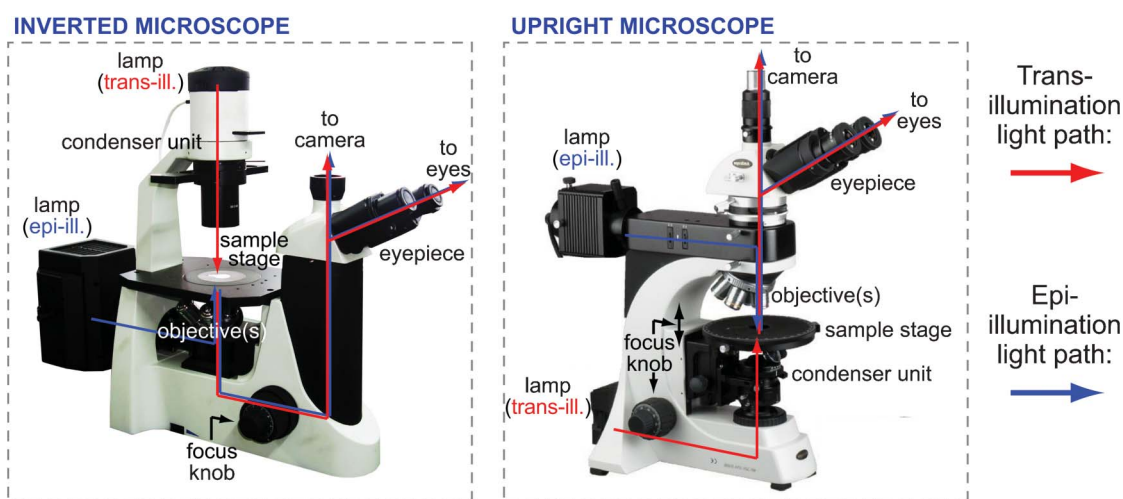


Fig. 3 Photos of two standard compound microscopes: An inverted microscope (left) and an upright microscope (right) compatible with both bright-field and fluorescence microscopy. The red and blue light rays show the paths for trans-illumination and epi-illumination microscopy, respectively.

illuminated. The standard illumination technique in wide-field microscopy is called Köhler illumination.⁹ The basic idea of Köhler illumination is to provide a uniform illumination of the specimen. This is achieved by a series of optical elements and a collector–condenser system which are aligned so that the image of the light source (*e.g.*, the filament of a halogen lamp) is maximally defocused in the specimen plane. In Fig. 2, this can be seen by following the light rays from two different points in the light source (here, a spiral-shaped lamp filament). At any point where the pair of dotted or solid lines converges, an image of the light source is formed. In the trans-illumination microscope, three such images (“lamp images”) are formed between the light source and the detector. The specimen itself is located in between two such lamp images, causing rays from a single point in the lamp filament to fill out the whole field of view in the specimen plane. Simply speaking, we have achieved a maximally blurred lamp image in the specimen plane. However, illumination uniformity is not the only important parameter in wide-field microscopy; the Köhler arrangement provides the operator with additional degrees of freedom for control. In the specimen plane, it is possible to control the illuminated area, the light intensity and the solid angle under which the specimen is illuminated (*i.e.*, the “diffusivity” of the illumination). This is achieved by adjusting the apertures of

two diaphragms in the collector–condenser system and is of particular importance for different contrast-enhancing techniques discussed later (Section II C).

An alternative to trans-illumination is epi-illumination (*cf.* mid-left part of Fig. 2). In this mode, the light from the specimen is collected and detected from the same side as where the sample is illumination. This is a common method when studying non-transparent (scattering/reflecting) objects such as a printed circuit board or when using fluorescence. In microfluidics, many microchips are not transparent making this illumination mode the only possible alternative. In fluorescence microscopy, epi-illumination facilitates the separation of excitation light from fluorescence emission. To accomplish epi-illumination, a beam splitter is used to separate light from the light source and from the specimen. The beam splitter is either a semi-transparent mirror (in bright-field epi-illumination microscopy) or a filter cube comprising a dichroic mirror and a set of optical filters (in epi-fluorescence microscopy). The dichroic mirror is designed to reflect short wavelengths (the excitation light) and transmit long wavelengths (the emission light).

It is possible to combine trans-illumination and epi-fluorescence in real time by operating the two illumination systems simultaneously. An example is shown in Fig. 4, where a cluster of cells trapped in an ultrasonic “cage”^{10,11} is

viewed in epi-fluorescence mode (Fig. 4a), trans-illumination bright-field mode (Fig. 4b) and finally in combined mode (Fig. 4c). The combined mode clearly reveals which of the cells in the cluster are labeled with green fluorescence. In this case the green cell is a human embryonic kidney (HEK) cell labeled with calcein-AM, which is trapped in a cluster of natural killer (NK) cells. This mode of microscopy is particularly useful, for example, to simultaneously image the microfluidic device structure (*e.g.* channels) and objects (*e.g.* cells) within the device. However, this only works for strongly fluorescent samples as the fluorescence must be clearly distinguishable from the bright background. In high-sensitivity, quantitative fluorescence applications, any background light must be carefully suppressed.

A. Magnification. A modern research microscope is built up with several modules and is called a compound microscope. The first and most important choice when setting up the microscope is the choice of objective. Often a number of different objectives are mounted in a rotatable objective turret. Objectives are made with different properties. The most obvious to a user is the magnifying power (typically between $1\times$ and $100\times$). The magnified image is viewed through an eyepiece which typically magnifies the image another $10\times$,

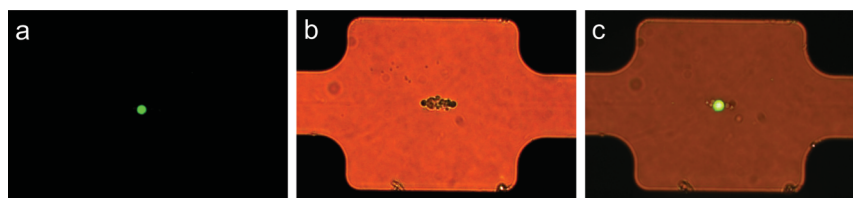


Fig. 4 Practical examples of different illumination techniques in optical microscopy. (a): Epi-fluorescence microscopy. (b): Trans-illumination bright-field microscopy. (c): Combined epi-fluorescence and trans-illumination bright-field microscopy. The sample is an aggregate consisting of one human embryonic kidney (HEK) cell labeled with the green-fluorescent viability assay calcein-AM and approximately eight natural killer (NK) cells. The cell cluster is trapped and retained in a flow in an ultrasonic cage, which is described in more detail in Ref. 11.

or is detected by a camera by projecting the image onto a CMOS or CCD chip with the help of an adapter lens. The adapter lens adjusts the size of the projected image to cover the full size of the camera chip, normally magnifying between $0.5\times$ and $2.5\times$. The total magnification is given by the product of the objective's magnification and the eyepiece's or camera adapter's magnification.

When the specimen is viewed directly through the eyepiece, magnification refers to the viewing angle. Thus, the standard definition of the total magnification of a microscope is to compare the apparent angle the specimen is covering viewed through the eyepiece compared to the corresponding angle when viewed by the naked eye at a distance of 25 cm. In the case of camera detection, the concept of total magnification is simpler since it can be directly related to the size of the CCD chip in the camera (*i.e.*, viewing angle is not relevant in this case). When choosing a camera, the pixel number is not the most important for the resolution. Instead, it is the pixel size that needs to be matched with the optical resolution of the microscope, *cf.* Section II B. In particular, note that higher magnification does not automatically lead to higher resolution. Instead, it is the light collecting angle and the aberrations of the objective that determines the resolution. This is discussed in Section II B. Another important matter when using a camera is to choose a suitable camera adapter. In microscopy, the camera adapter corresponds to the camera lens used for normal photography. Most microscope objectives are designed to provide a field of view in the image plane between 20–25 mm. However, the CCD chip in the camera is often smaller, typically in the range 5–10 mm wide. Therefore, camera adapters often have

$0.5\times$ magnification to reduce this mismatch. If the CCD chip size is known, the field of view in the camera image can easily be calculated by dividing the CCD chip size with the total magnification, see example in Table 1.

B. Resolution. After magnification, the next important property of the objective is the numerical aperture (N.A.). This is a measure of the objective's maximum resolving power and is defined as:

$$\text{N.A.} = n \sin \alpha \quad (1)$$

where n is the refractive index of the immersion medium between the specimen and the objective, and α is half the maximum light-collecting angle of the objective (*cf.* Fig. 2).

For a given N.A., the diffraction-limited resolution can be estimated from the Rayleigh criterion as:¹²

$$D = \frac{0.61\lambda}{\text{N.A.}} \quad (2)$$

where D is the smallest resolvable distance between two closely lying point sources (or details) in the object, and λ is the wavelength of the emitted light from the object. Thus, the resolution of the microscope is dependent on n , α and λ . From eqn (1) and (2), we see that the resolution can be increased by using high-index immersion medium, n (*e.g.* water or oil instead of air), by increasing the light-collecting angle of the objective, α , and by using short wavelength light, λ . The N.A. (*i.e.*, n and α) is normally defined by the design of the objective where the size of the front lens, the working distance and the immersion medium are fixed parameters. The working distance is often marked with “WD” on the objective. Typically, high-N.A. objectives have short working distances

in order to increase the light-collecting angle. When imaging a closed microfluidic device, it is important to use an objective with a sufficiently long working distance so that the full depth of the device (*e.g.* its microchannel) can be placed in focus, *i.e.* imaged sharply. It is important to note here that objectives are often designed to work with a certain coverslip thickness, *i.e.* the lid of the microfluidic device. The coverslip can actually be considered as a component of the objective and wrong coverslip thickness will degrade performance significantly. The majority of all objectives are made for borosilicate coverslips #1.5, *i.e.* a thickness of 150–190 μm . This is discussed in more detail in Section IV. Objectives with different magnification and N.A. are listed in Table 1, together with microfluidic application examples.

As a practical example of diffraction-limited resolution (*cf.* eqn (2)), an object viewed with blue light (*e.g.* the blue line of an argon-ion laser, $\lambda = 458 \text{ nm}$) through a high-index oil-immersion objective (*e.g.* N.A. = 1.4) results in $D = 200 \text{ nm}$. This is roughly the maximum resolution that can be achieved with a standard optical microscope and visual light. An example of the Rayleigh resolution criterion is shown in Fig. 5, which illustrates the predicted (Fig. 5a–c) and real (Fig. 5d) diffraction-limited images of point-like objects (*e.g.* sub- μm fluorescent beads). However, note that the definition in eqn (2) provides no information about the smallest detectable object. For example, a fluorescent bead with size much smaller than D can still be visible in a standard optical microscope given that it is bright enough relative to its background and that it does not move too much. This results in an imaged spot (called Airy disc) having a radius $r_{\text{spot}} = D$ (*cf.* Fig. 5a and 5c). In Fig. 5d, real microscope images of green-fluorescent

Table 1 Magnification and numerical aperture of objectives commonly used in microfluidics

Magnification	Typical numerical aperture (N.A.)	Approx. resolution (D)	Approx. depth of field	Typical working distance	Approx. field of view (in camera image) ^a	Application example in microfluidics
1 × –1.25 ×	0.025–0.03 (dry)	>10 μm	600–900 μm	3–4 mm	11–14 mm	Imaging a whole micro-fluidic chip of size >1 cm
2.5 ×	0.075 (dry)	4 μm	100 μm	6–15 mm	5.6 mm	Imaging sharply in a 100 μm deep channel
5 ×	0.12–0.16 (dry)	2–3 μm	20–40 μm	10–20 mm	2.8 mm	Intermediate resolution with good field of view, long working distances available
10 ×	0.20–0.50 (dry)	0.7–1.7 μm	2–14 μm	2–16 mm	1.4 mm	Very good trade-off between resolution and field of view
20 × –25 ×	0.30–0.80 (dry) 1.0 (water)	0.3–0.8 μm	0.5–3.4 μm	0.2–12 mm	500–700 μm	Often sufficient resolution (sub-μm) in many applications
40 ×	0.65–0.9 (dry) 1.0–1.2 (water) 1.3–1.4 (oil)	0.2–0.5 μm	0.3–1.3 μm	0.16–2 mm	350 μm	Best resolution and performance, good for single-cell imaging
100 ×	0.65–0.95 (dry) 1.0–1.25 (water) 1.25–1.46 (oil)	0.2–0.5 μm	0.3–1.3 μm	0.1–1 mm	140 μm	Similar performance as for 40 × objectives

^a Estimation of the scale of the longest width in the camera image based on the following assumptions: 7 mm wide CCD chip and a 0.5 × camera adapter. This corresponds to a 14 mm wide image before the camera adapter, which must be smaller than the specified field of view of the objective (typically between 20–25 mm).

200 nm and 500 nm beads are shown to verify the predicted images in Fig. 5a–c. The images in Fig. 5d are acquired with a 100 × dry-immersion objective with N.A. = 0.95. Using eqn (2), the diameter ($d = 2r_{\text{spot}} = 2D$) of the imaged spot from a point source is equal to 660 nm (for $\lambda = 515$ nm and N.A. = 0.95). Since this lower limit is larger than both 200 nm and 500 nm, we can expect that the imaged spots of 200 nm beads and 500 nm beads will not differ much in size. This is verified in Fig. 5d, where the image of the 500 nm bead is only about 20% wider than the image of the 200 nm bead. If diffraction was the only limiting

factor, theory predicts about 30% difference in imaged widths under these circumstances.

Another important effect of high-resolution imaging is the short depth of field for high-N.A. objectives. Depth of field is defined as the thickness of the layer where the specimen is imaged sharply. This thickness is proportional to $\lambda/\text{N.A.}$ ^{2, 12} which means that for the objective and fluorescence color in Fig. 5d the depth of field is approx. equal to the bead size (500 nm). As a result, a 500 nm bead vertically displaced on the order of 1 μm is imaged as in Fig. 5d, lower panel. In microfluidics,

objectives with high N.A. should only be used if the sample is positioned with μm-precision, preferably on the bottom of the channel. This is further discussed in Section IV.

The Rayleigh criterion can be used to estimate the maximum resolution that can be achieved with a chosen objective. This is a fundamental limit originating from the wave nature of light. However, in reality other engineering-related limitations often define the image quality and resolution, in particular for less expensive objectives. These limitations are called aberrations, and are summarized in Table 2. In general, an optical

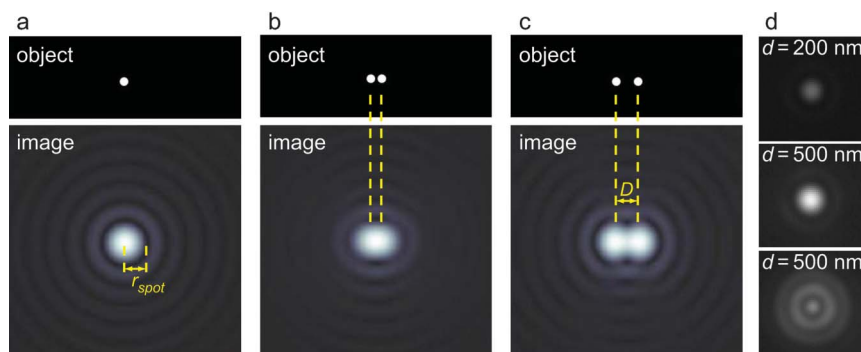


Fig. 5 (a–c): Conceptual-model illustration of the Rayleigh criterion for the minimum resolvable distance, D , between two small point-like objects. (a): The diffraction-limited predicted image (lower panel) of a small object (upper panel) consisting of a bright sphere. (b): The corresponding image of two such small spheres, unresolved case. (c): Same as in (b) but the limit where the spacing, D , is just large enough for resolving the two small spheres. The radius of the imaged spot, r_{spot} , in (a) is equal to the minimum resolvable distance, D , in (c). The situation in (c) illustrates the Rayleigh criterion. This criterion is defined as when the first intensity minima from the center of the imaged spot from one of the objects coincides with the intensity maxima of the other object, *i.e.*, when $D = r_{\text{spot}}$. (d): Real microscopy images of a 200 nm fluorescent bead (upper panel) and a 500 nm fluorescent bead (middle and lower panels) acquired with a 100 ×/0.95 (magnification/numerical aperture) objective. The upper and middle panels show the images of the beads in the focal plane, while the lower panel shows the effect of imaging a bead slightly out-of-focus.

Table 2 Objective classes (corrections for aberrations)

Name	Correction	Typical use	Relative price (ranging from about 100 Euro to 10 000 Euro)
Achromat	Color-corrected, narrow band	Basic visual inspection	\$
Plan achromat	Color-corrected, narrow band, field curvature correction	Basic visual inspection, need for sharp images within the whole field of view, and photographic recording	\$\$
Fluorite	Color-corrected, intermediate band	Suitable for fluorescence applications with short-wavelength excitation	\$\$\$
Plan fluorite	Color-corrected, intermediate band, field curvature correction	Suitable for fluorescence applications with short-wavelength excitation, need for sharp images within the whole field of view, and photographic recording	\$\$\$\$
Apochromat	Color-corrected, wide band	Suitable for demanding applications, typically high-resolution multiple-probes fluorescence	\$\$\$\$\$
Plan apochromat	Color-corrected, wide band, field curvature correction	Suitable for demanding applications, typically high-resolution multiple-probes fluorescence, need for sharp images within the whole field of view, and photographic recording	\$\$\$\$\$\$

aberration is any type of deviation in the imaging performance of an ideal lens or lens system. Such a deviation originates from rays passing through the periphery of a lens and/or at a large angle relative to the optical axis. Thus, while the definition of N.A. suggests the use of large-diameter lenses and wide-angle light cones, aberrations typically increase with lens diameter and light angle. Still, even small lenses are not aberration-free. The solution is to correct as many aberrations as possible by using complex lens systems containing combinations of several lenses and lens compounds (doublets and triplets) with up to 15–20 lens elements in total for advanced objectives. Table 2 lists different aberration-corrected objective classes, together with their performance and relative cost. All modern objectives are corrected for spherical and chromatic aberration to some extent, but more expensive objectives are better corrected for chromatic

aberrations and also for field curvature. The latter is important when imaging at high resolution over a broad spectral range and in a wide field of view, *e.g.*, in fluorescence microscopy and when recording images with a sensor. A final note about aberrations is that a glass layer between the objective and the specimen can act as a source of spherical aberration. As previously discussed, objectives are often designed for 150–190 μm borosilicate coverslip use. Thus, this is the optimal material and thickness of a glass layer for sealing of a microfluidic channel. If another thickness and/or material are used, an objective with a correction collar should be used for optimal microscopy performance.

When using microscopy in an acoustofluidic micro-device, the choice of objective should be matched with the illumination and detection systems, with the properties of the specimen/sample, and with the micro-device. An example

of this is shown in Fig. 6, where a $375 \times 110 \mu\text{m}^2$ (width \times height) transparent acoustofluidic channel filled with a suspension of $4.5 \pm 0.7 \mu\text{m}$ polyamide beads (“blood-mimicking fluid”, Danish Phantom Design, Denmark) and actuated at 5.68 MHz is imaged in transillumination mode with two different objectives: One with N.A. = 0.075 and one with N.A. = 0.30. First, we notice that the pattern of aggregated beads in the pressure nodes of the acoustic standing wave is clearly resolved in both cases. However, single-bead resolution and identification is only possible in Fig. 6b. Note that the field of view relative to the resolution and camera pixel size is well matched in both cases: The theoretical radius of the imaged spot from a point source, r_{spot} , (*cf.* eqn (2)) is approximately equal to the pixel size in both Fig. 6a ($r_{\text{spot}} \approx \text{pixel size} \approx 4 \mu\text{m}$) and in Fig. 6b ($r_{\text{spot}} \approx \text{pixel size} \approx 1 \mu\text{m}$). Thus, in this experiment, the digital resolution

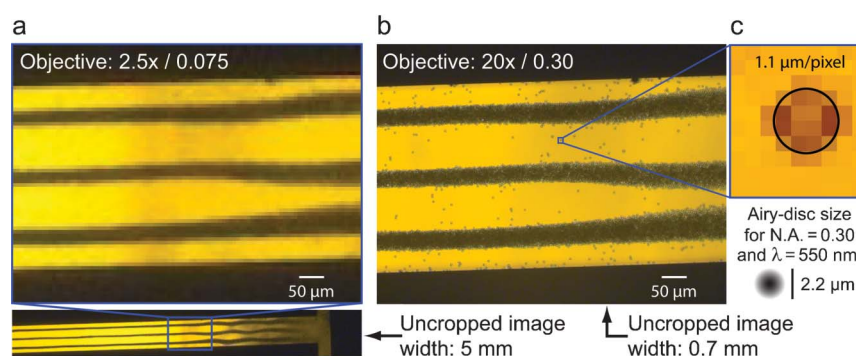


Fig. 6 Comparison between images acquired with (a): A $2.5 \times / 0.075$ (magnification/numerical aperture) objective and (b): A $20 \times / 0.30$ objective. The image in (a) is cropped to match the scalebar in the image in (b). (c) Zoom-in displaying the image of a single $4.5 \mu\text{m}$ diameter polyamide bead, including the pixel size and the theoretical diffraction-limited image of a point source (the Airy disc) for N.A. = 0.30 and $\lambda = 550 \text{ nm}$. The circle indicates the size of a $4.5 \mu\text{m}$ diameter circle scaled by the use of the channel width ($375 \mu\text{m}$) as a reference. The images show the pattern of beads undergoing acoustophoresis at the ultrasonic frequency 5.68 MHz in a $375 \times 110 \mu\text{m}^2$ (width \times height) microchannel.

(pixel size) is matched to the optical resolution (r_{spot}). As expected, the ratios of these resolutions ($r_{\text{spot},c}/r_{\text{spot},b} = 4$ and pixel size_c/pixel size_b ≈ 4) both correspond to the ratio of the numerical apertures ($\text{N.A.}_b/\text{N.A.}_c = 4$). Furthermore, if we need to image and identify single beads of size 4–5 μm , the imaging performance in Fig. 6a is not sufficient; we need at least ~ 5 times better optical and digital resolution relative to the bead diameter to correctly identify single beads (*cf.* Fig. 6c). This is provided that all beads are in the focal plane of the objective, *i.e.*, that the depth of field is large enough. However, if we take into account the sampling theorem¹³ and compare with eqn (2), the pixel-to-pixel distance should not be more than $0.4 \times D$ in order to avoid subsampling. For the objective used in Fig. 6b ($\text{N.A.} = 0.30$), the depth of field is roughly about the same size as the bead diameter (*cf.* Table 1). This indicates that most beads in Fig. 6b are located on the channel bottom. If beads are uniformly distributed in a $\sim 100 \mu\text{m}$ high channel, an objective with slightly lower magnification and N.A. than in Fig. 6b is a better choice, *e.g.* a $10 \times /0.25$ objective as used in Ref. 14.

C. Contrast. Contrast is an important parameter to consider when imaging a microfluidic channel, in particular when the specimen is a water-based cell suspension. Cells are difficult to distinguish from water because they have high water-content and are highly transparent. Optically, this means that cells have a refractive index, n_{cell} , close to the refractive index of water, n_{water} . As a result, light rays are neither deflected nor reflected by the cell to any significant extent. Thus, the image of the cell suspension may appear as pure water. Two different strategies can be used to overcome this problem: Either to stain the cells with a color substance or fluorescent probe, or to use an optical method to enhance the natural contrast between cells and suspension medium. Fluorescence microscopy is discussed in Section III B while bright-field-based techniques for contrast enhancement are discussed in Section III A. The latter includes phase contrast, dark field and differential interference contrast (DIC).

D. Light sources and detectors/cameras. The standard light sources in a compound microscope are a halogen

lamp for bright-field microscopy, a mercury-vapor lamp or LED for (wide-field) fluorescence microscopy, and lasers for (laser-scanning) confocal fluorescence microscopy. In Fig. 3, a mercury lamp is used for epi-illumination, and a halogen lamp is used for trans-illumination. Mercury lamps have higher efficiency than lamps of incandescent filament-type such as the halogen lamp. However, they are not as flexible in start-up time and intensity adjustments as the halogen lamp. In addition to its high intensity, mercury lamps have a strong emission in the lower wavelength regime (*i.e.*, near-UV, blue and green). Since the mercury lamp spectrum consists of several peaks and valleys, optical filters are often matched with the fluorophores used enabling simultaneous detection of fluorescence (*cf.* the “filter cube” in Fig. 2). In recent years, LED’s have become an attractive alternative to mercury lamps based on their long life time and low heat dissipation.

The standard detectors are a CCD or CMOS camera in wide-field microscopy, and a photo-multiplier tube (PMT) in confocal microscopy. Note that a PMT is a single-element detector that requires a serial scanning procedure for generating an image, rendering confocal microscopy a rather slow technique. On the other hand, a PMT can be more sensitive than a CCD although today CCDs are sufficiently sensitive for most applications.

III. Modes of optical microscopy

In this section we discuss different modes of optical microscopy that are used when imaging acoustofluidic micro-devices. The typical specimen in these devices is either cells or polymer beads suspended in a water-based fluid inside a micro-channel or micro-chamber. Although the examples are chosen from acoustofluidic devices, the discussions are relevant for any type of micro-device of similar design.

A. Bright-field microscopy

Bright-field is the basic mode of microscopy where the specimen is viewed with white-light illumination and contrast is provided naturally by a combination of transmission, reflection, refraction, scattering and absorption mechanisms. The name refers to the bright background

seen around a shadowing object. However, due to the low contrast when imaging cells, bright-field microscopy is often operated in a contrast-enhancing mode. The three most important modes are phase contrast, dark field and differential interference contrast (DIC). These contrast methods are typically performed in trans-illumination mode.

A1. Phase contrast. This method utilizes the phase difference introduced by a ring-shaped phase plate between scattered and unscattered rays. The phase plate is combined with a ring aperture in the condenser that gives cone-shaped illumination of the specimen. In this way, rays that are unscattered pass through the ring part of the phase plate, while scattered rays pass through other parts of the phase plate (having a different thickness than the ring part). Interference between these rays increases the contrast between the image background and the specimen (*e.g.* the structures of a cell). In practice, the phase plate is integrated in the objective, which is marked with “Ph” or similar. Thus, an objective specifically designed for phase contrast is needed. Furthermore, a ring aperture needs to be inserted and aligned in the condenser system. Another remark is that optimal contrast is achieved for the phase difference $\pi/2$ between the scattered and unscattered rays. Exactly this shift can only be generated for one wavelength, hence, the optimal effect is achieved with monochromatic light (typically green light around 550 nm). However, phase contrast can also be performed with good results with white light. It should be noted that a common artifact in phase contrast images is a halo around objects such as a cell. Furthermore, the best effect is achieved for thin and transparent samples such as a monolayer of cells. An example of phase contrast imaging of a monolayer of cells aggregated and trapped by ultrasound in a half-wave microfluidic channel is seen in Fig. 7b and compared with standard bright-field imaging in Fig. 7a.

A2. Dark field. This is a rather straightforward and useful method to discriminate between direct (unscattered) rays and rays scattered by the object and is particularly suitable for weakly

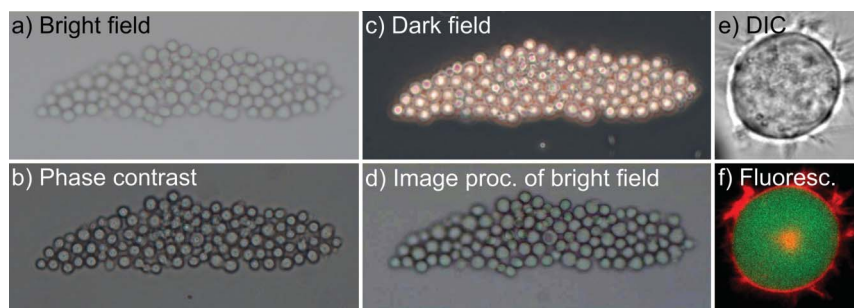


Fig. 7 Ultrasonically trapped cells imaged with different contrast modes: Bright field (a), phase contrast (b), dark field (c), digital image processing of the bright field (d), differential interference contrast (e) and dual-color fluorescence (f). The cells in (a)–(d) are COS-7 cells, and in (e)–(f) a human B cell.

scattering objects and for low-concentration samples of small particles. Just as with phase contrast, this method utilizes a ring aperture in the condenser system to produce cone-shaped illumination. However, instead of a phase plate, dark field imaging uses a condenser with higher N.A. than of the objective. This, together with a suitable ring aperture alignment, causes unscattered rays to completely miss the objective. For cell imaging, the result is bright cell structures on a dark background which may reveal slightly different image information compared with, *e.g.*, phase contrast images. No particular objective is needed for dark field imaging, as long as its N.A. is lower than the N.A. of the condenser. An example of dark field imaging is shown in Fig. 7c (same object as in Fig. 7a–b). When using a stereo microscope with a flexible-arm illumination, a dark-field effect can be achieved by adjusting the arm into a suitable oblique illumination angle relative to the specimen plane.

A3. DIC. Differential interference contrast (DIC) microscopy, or Nomarski microscopy, is based on imaging local gradients in optical path lengths in a sample by the use of polarized light. A simplified description of the method is as follows: Linearly polarized light is split by a so called Wollaston prism into two differently polarized and laterally displaced beams. These beams pass through the sample. A second Wollaston prism then recombines the beams and they are filtered by a second polarizer (analyzer). Interference between the recombined beams after the second polarizer produces an image where small local variations in refractive index of the sample are

enhanced, see example in Fig. 7e. The variations are in the displacement direction defined by the orientation of the Wollaston prisms, which can be adjusted by the operator. It should be noted that the DIC images of, *e.g.* a cell, often appear as relief-type images which should not be mistaken for topological details. Although useful, DIC images are not always easy to interpret. In practice, DIC microscopy is useful for thicker samples and doesn't suffer from the halo effect seen in phase contrast imaging. In microfluidics, DIC cannot be used with plastic devices since the birefringence of plastics destroys the DIC effect. Thus, plastics are perfect depolarizers. The optimal device material for DIC is glass. Care should also be taken when clamping a glass chip in a chip holder, since induced stresses also causes depolarization.

B. Fluorescence microscopy

Fluorescence microscopy is a sensitive and useful technique allowing quantitative analysis of cells or other objects with high contrast and selectivity.¹⁵ The light source in the microscope system, typically a mercury arc lamp or a laser (*cf.* Fig. 2 and 3), is used to transfer fluorophores to the excited state and fluorescence can then be collected by the microscope detector system. The fluorescence light is most often of a longer wavelength (redshifted) compared to the excitation light and is emitted incoherently in all directions independently of the direction of the excitation light. To minimize contaminating light from the excitation source, fluorescence is typically detected in the opposite direction from the excitation (*i.e.* in epi-illumination mode) and through a filter only allowing passage of red-shifted photons

(*cf.* filter cube in Fig. 2) and not back-scattered excitation light.

B1. Fluorescent probes. The chemical structure largely determines how efficiently and at what wavelength the molecule absorbs and emits light. The molecular extinction coefficient is a measure of the absorption and the quantum yield specifies what fraction of the relaxation back to the ground state takes place through fluorescence. Thus, both of these parameters should be high for efficient fluorescence. Some fluorophores have a fluorescence quantum yield that is sensitive to the local micro-environment and can be used as sensors for *e.g.* pH or Ca^{2+} concentration. Several molecules occurring naturally in cells absorb UV light, but the abundance of cellular molecules absorbing visible light (400–700 nm) efficiently is relatively low. This provides a spectral window where cells are largely transparent and also non-fluorescent. This window can be utilized for fluorescence microscopy by using fluorophores that are excited by visible light. Typically, such molecular probes are rather small polyaromatic hydrocarbons or heterocycles and, thus, much smaller than many biomolecules, *e.g.* proteins. By chemical modification of the fluorophores, both their fluorescent properties, *e.g.* wavelength or excited-state lifetime, and intracellular localization can be tuned.

B2. Cellular labeling with fluorescent probes. It is important to consider what property of the cell need to be analyzed when selecting a fluorescent probe. If the purpose is to detect cells or distinguish different populations of cells there are several tracking dyes available. Such dyes

typically distribute in the cellular cytoplasm (*e.g.* calcein-AM), bind covalently to intracellular proteins (*e.g.* CFSE), or accumulate in the plasma and intracellular membrane of cells (*e.g.* DiO). Such dyes often stain cells brightly and are available in a variety of colors.

A widely used technique for fluorescent detection of specific proteins is to use antibodies. Antibodies can either be directly labeled with the fluorophore of choice or combined with secondary fluorescently-conjugated antibodies that bind to the first (primary) antibody. The advantage of using secondary antibodies is that the library of primary antibodies can be kept lower as there is no need to maintain the same antibody directly labeled with different fluorophores. When using antibodies it is important to keep track of which species the antibody was raised in and care should be taken to use appropriate controls with non-specific antibodies of the same isotype. If the antibody binds non-specifically to cells erroneous conclusions can be drawn about the protein distribution and quantity.

Molecular biology can be used to introduce fluorescent proteins, *e.g.* green fluorescent protein (GFP), into cells and is an excellent strategy for many imaging applications, in particular for live cell imaging. Some drawbacks are that it can be time consuming or difficult to generate cells expressing the protein of interest, especially if one wants to use primary cells. Other limitations are that the GFP-tag may affect the natural distribution and behavior of the protein of interest, and the fact that the vectors carry different promoter regions (*i.e.* specialized DNA sequences where the transcription process starts) compared to the wild-type DNA. This often leads to protein overexpression, which facilitates detection but may affect the natural function and localization of the protein. Despite those limitations and concerns, the use of GFP is now the predominant approach for introducing fluorescence in live cell applications.

B3. Live-cell fluorescence microscopy.

Live cell imaging poses some additional challenges since the cells generally need to be maintained in culture medium and a physiological atmosphere (37 °C and humidified air complemented with 5%

CO₂) if they are to be imaged for long times. There are different approaches to create chambers allowing control of the environment around the cells while imaging. Two common ways are to either place the cells in a rather small heating block that is placed on top of the microscope stage or to encapsulate the whole microscope stage in a larger chamber where the atmosphere is kept at the desired level. For both approaches it is common to have a supply of humidified air supplemented with 5% CO₂ that purge the cells. Cells can survive at lower temperature in a buffered environment for limited times but it should be remembered that dynamic cellular processes are temperature dependent. One cannot expect that the rate of enzymatic activity, molecular transport or diffusion will be the same at lower temperature.

Another challenge in live cell imaging is that many fluorescent probes that stain fixed cells cannot be used to efficiently stain live cells. Major reasons for this are that many probes do not easily cross the plasma membrane of live cells or that they are toxic to cells, sometimes increasingly so during imaging due to formation of reactive oxygen species. Despite these limitations, there are several probes that are useful for live cell imaging in addition to fluorescent proteins (discussed in the previous section). Examples are found among cytoplasmic dyes, lipid dyes and some nuclear dyes. As a general rule, one should strive to use as small a dye concentration as possible for live cell imaging and, if possible, use experimental controls that probe if normal cellular function is maintained also when the cells are stained.

The fact that the plasma membrane provides a natural boundary that is difficult for some molecules to cross can be used to design different labeling strategies. For example, dead cells can be distinguished since some dyes can only leak through the compromised plasma membrane of a dead cell and not the intact membrane of live cells.¹⁶ This can be exploited by use of dyes that leaks out from the cell or into the nucleus as it dies. Examples of viability probes suitable for acoustofluidic cell handling are provided in Ref. 16.

B4. Multiple fluorescent probes. When selecting probes for cellular experiments,

the choice of fluorophores needs careful consideration, taking into account their individual absorption and emission spectra as well as the properties of the imaging system used. Even if modern high-end confocal microscopes often are equipped with multiple laser lines for excitation and several detectors combined with tunable filters, it is generally difficult to image more than 3–4 dyes in the same sample without getting unwanted fluorescence bleed-through or cross talk between the channels. To limit the cross talk it is desirable to use dyes with narrow fluorescence spectra. An example of a dual-labeled cell trapped by ultrasound is seen in Fig. 7f.

B5. Optical sectioning techniques. It is sometimes desirable to get three-dimensional information about the sample studied and the quality of that information depends heavily on the imaging system. With a conventional fluorescence microscope, the resolution along the optical axis is generally quite poor. However, when using a technique allowing optical sectioning (such systems include laser-scanning confocal microscopy, spinning-disc confocal microscopy, structured-illumination microscopy and two-photon microscopy)¹⁷ the quality of the 3-D information can be much higher, especially if a 3D reconstruction is made in specialized software. However, this requires multiple acquisitions, which obviously leads to longer imaging time. Furthermore, if the imaged objects move between sequential images, significant distortions in the 3D reconstructed image can occur.¹⁸ Distortions due to cell drift can be corrected for, but morphological changes of a cell during acquisition are more difficult.

IV. Implementation of optical microscopy in an acoustofluidic micro-device

In this section we discuss how to design an acoustofluidic micro-device intended for use in an optical microscope (Section IV A). The discussion includes choices of materials and dimensions, how to match the device with a certain objective and illumination method, and how to match the acoustic performance with the optical performance. Finally, we provide examples of applications of acoustic manipulation of

cells in micro-devices characterized by optical microscopy (Section IV B).

A. Design criteria

A microfluidic chip used for acousto-phoresis has carefully selected thicknesses and materials of the supporting structures, in order to host and control acoustic resonances. The typical chip design is a half-wave fluid channel surrounded by an acoustically hard material such as silicon or glass.¹⁹ Glass has optimal material properties for both hosting acoustic resonances, as well as for high-resolution optical microscopy. A polymer material is a less suitable choice for two reasons: (1) its high acoustic absorbance, and (2) its optical birefringence (which makes DIC microscopy impossible). Therefore, most acousto-phoresis chips use a combination of glass and silicon: glass for optimal visual access and silicon for optimal channel processing. If the supporting structures around the fluid channel have thicknesses corresponding to an odd multiple of a quarter wave in that material, the design is a layered resonator.²⁰

A suitable starting point when building a layered acoustic resonator compatible with high-resolution microscopy is to use

the same materials and thicknesses as established as a microscopy standard: A $170 \pm 20 \mu\text{m}$ thick borosilicate layer (*i.e.*, a standard coverslip) and a 0.8–1.0 mm thick borosilicate layer (*i.e.*, a standard microscope slide, typical dimension $25 \times 75 \text{ mm}^2$ or $1 \times 3 \text{ inches}^2$). If other glass materials than borosilicate are used, the refractive index, n , should preferably be as close as possible to the index of borosilicate (*i.e.*, n between 1.51 and 1.54). By proper acoustic frequency selection, the thinner glass layer can act as an acoustic quarter-wave reflector on the side of the chip facing the microscope objective. For example, a $170 \mu\text{m}$ thick Pyrex layer (one type of borosilicate glass) has a quarter-wave resonance frequency of about 8.3 MHz (given a speed of sound = 5661 m s^{-1}).¹⁹ This resonance frequency defines the driving frequency of the transducer, which, in turn, defines the half-wave thickness of the water-filled fluid channel to about $90 \mu\text{m}$ (given a speed of sound = 1497 m s^{-1}).¹⁹ The other reflecting layer on the opposite side of the channel should preferably be thicker than a quarter-wave, otherwise the total stack of layers will become fragile. Two options are available: Either to use a two-layer chip

with the channel etched in silicon or glass and closed by a glass layer, or to use a three-layer chip with the channel etched throughout the mid-layer.²⁰ The latter is the most flexible since the channel can be etched in any material and then closed by two glass layers. Furthermore, this option also makes it possible to use the standard coverslip/microscope slide combination for the two glass layers building up the micro-device. This is important since all microscope suppliers have designed their microscope components to be compatible with these materials and dimensions: A coverslip facing the objective and a glass slide facing the condenser system. Thus, using the $170 \pm 20 \mu\text{m}$ and 0.8–1.0 mm combination for the glass layers will result in a chip compatible with both high-Q acoustic resonances and any type of optical microscopy (both epi- and trans-illumination). In theory, the optimal choice is $170 \mu\text{m}$ and $850 \mu\text{m}$. This is exactly equivalent to $\lambda/4$ and $5\lambda/4$ acoustic reflectors at 8.3 MHz, which perfectly matches the microscopy coverslip/glass slide standards.

If the mid-layer in between the two glass layers is silicon, acoustic resonances can also be built up in the transversal direction perpendicular to the layered

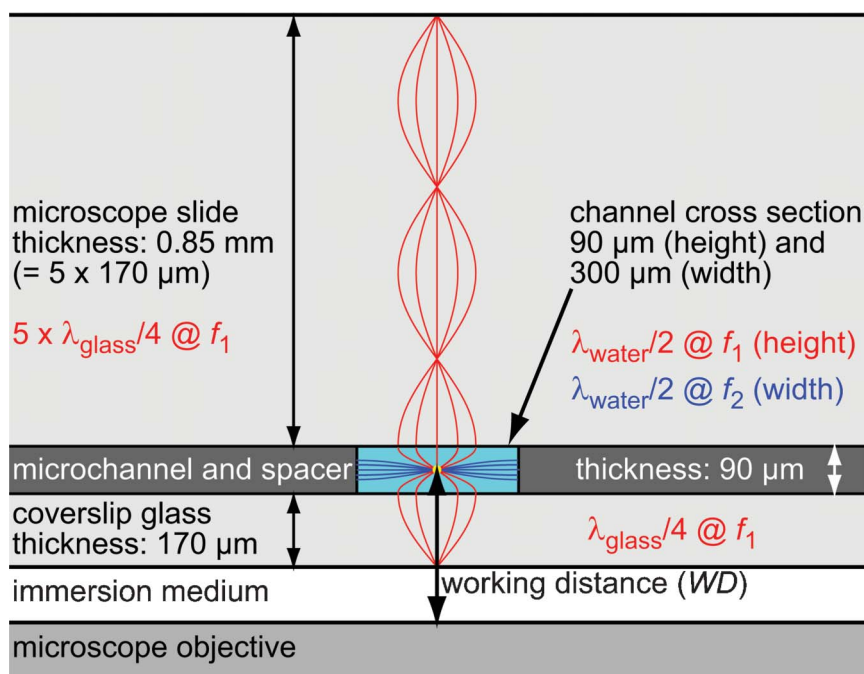


Fig. 8 An optimized design of a layered acoustic resonator for 2D ultrasonic manipulation in the fluid channel, compatible with high-resolution optical microscopy. The chip is a three-layer structure based on a coverslip glass (bottom) and a microscope slide glass (top). A spacer layer is sandwiched in between the two glass layers defining the channel height. The chosen thicknesses correspond to a vertical resonance frequency f_1 of 8.3 MHz, and a horizontal resonance frequency of another lower frequency defined by the channel width (*e.g.* 2.5 MHz for the width $300 \mu\text{m}$).

resonator enabling three-dimensional acoustic particle manipulation.¹⁰ This design is a hybrid between the layered resonator and the transversal resonator described in Ref. 20. An example of such a layered/transversal resonator hybrid is seen in Fig. 8. A similar example is described in Ref. 10 and uses a 200 μm bottom layer in Pyrex, which is near but not fully optimized for high-resolution microscopy. Thus, the device is a three-layer chip compatible with both three-dimensional acoustic particle manipulation and trans-illumination microscopy. Here, a 110 μm thick silicon layer is sandwiched between two acoustic reflectors: A 200- μm ($\lambda/4$ -wave) Pyrex layer and a 1-mm ($5 \times \lambda/4$ -wave) Pyrex layer. Thus, the axial resonance (layered resonator) is around 7 MHz causing “levitation”²¹ of particles in the vertical direction, while the transversal resonances in the horizontal directions are defined by the channel width and length, respectively. High spatial control of the three-dimensional manipulation is achieved by implementing ultrasonic “cages” with half-wave dimensions along all the three dimensions width, height and length.¹⁰ Imaging of levitated particles and cells should be performed with an objective having a working distance of at least 200 μm + 55 μm (corresponding to the thickness of the bottom glass layer plus half the channel height).

The inverted microscope is the most convenient to use for imaging in a microfluidic chip, see Fig. 3. The inverted microscope has a beam line arrangement corresponding to flipping the schematic Fig. 2 vertically: The objective, epi-illumination source and the detector are below the sample stage, while the condenser system (*i.e.*, the trans-illumination source) is above the sample stage. This setup makes it possible to arrange all tubing, connectors, wires and ultrasonic transducers on the upper side of the microfluidic chip. This is particularly useful in high-resolution microscopy where high-N.A. objectives with short working distances are used. As previously mentioned, a closed microfluidic chip should preferably have a glass bottom layer (facing the objective in the inverted microscopy) of thickness near 170 μm . Furthermore, the objective used should be coverslip-corrected. This information is found in a second row below the magnification and N.A. labels on the

objective. For example, the label “ $\infty/0.17$ ” means infinity-corrected objective to be used with a glass coverslip of thickness 0.17 mm. This thickness is the most common standard in microscopy, sometimes called No. 1 $\frac{1}{2}$. Examples of other common labels are “ $\infty/0$ ” (no coverslip), “ $\infty/-$ ” (insensitive for coverslip) and “ $\infty/0.14-0.19$ ” (adjustable for different coverslip thicknesses). The latter type of objective with a correction collar is strongly recommended for use with microfluidic chips, since the chip layers may differ from the standard thickness of microscopy coverslips, or the glass material may have a different refractive index than the index of standard coverslips. The other label (“ ∞ ”) stands for infinity-corrected objectives, or infinity corrected system (ICS). This is the present standard for objectives, which means that the objective produces an intermediate image placed in infinity (in contrast to the older standard of 160 mm fixed tube length). The advantage with infinity-corrected objectives is the possibility to insert various optical components (such as filters, polarizers, beam splitters, *etc.*) in the optical path after the objective without causing image artifacts due to refraction. The ICS objectives are combined with a tube lens placed in between the objective and the eyepiece to relocate the intermediate image to a finite distance from the objective.

For high-resolution objectives with N.A. ≥ 1 , an immersion medium is always needed (*cf.* eqn (1)). This medium is oil, water, or, less common, glycerol. Oil-immersion is the best choice for thin microfluidic channels or in applications where only the channel bottom is imaged. Oil has the same refractive index as glass, which means that no refraction takes place between the cover slip and the objective. In principle, oil immersion objectives are insensitive for changes in the thickness of the glass layer. This means that any glass thickness shorter than the working distance of the objective can be used. On the other hand, refraction takes place between the coverslip and the fluid channel (given a water-based fluid inside the channel). This means that in applications where the object is located at a distance from the channel bottom, a water-immersion objective is a better choice. Thus, if water is the medium on both sides of the glass

layer, image distortion is minimized. In acoustofluidics, a vertically oriented half-wave channel used for trapping or aligning particles in the center of the channel should be imaged with a water-immersion objective if high-resolution microscopy is needed. However, it should be noted that the immersion medium will introduce acoustic transmission losses, which in turn may decrease the acoustophoresis performance. If a vertical resonance is used (*cf.* Fig. 8), dry objectives are the best choice.

B. Applications of microscopy to acoustofluidics

In this section we provide a few examples of acoustofluidic applications where optical microscopy is a central tool of the method. Fluorescence microscopy was used by Radel *et al.*²² to measure alterations in the vacuole structure of yeast cells exposed to ultrasound. Spengler *et al.*²³ performed quantitative measurements of the fractal perimeter dimension to investigate the morphology and stability of bead aggregates trapped by ultrasound in different solutions. The measurements were based on epi-illumination microscopy images. Quantitative fluorescence measurements were performed by Wiklund *et al.*²⁴ by the use of confocal laser-scanning microscopy (CLSM). They demonstrated a detection limit in the low femtomolar range for a bead-based human thyroid stimulating hormone (hTSH) assay by combining ultrasonic bead enrichment with high-sensitivity confocal fluorescence microscopy.²⁵ This work was performed in a standard 96-well plate. Bazou *et al.*²⁶ used both bright field and fluorescence microscopy to measure the rate of membrane-membrane spreading and the distribution of different trans-membrane proteins responsible for cell-cell adhesion in ultrasound-mediated aggregates of C6 neural cells. Similar measurements were also performed on prostate cell lines,²⁷ chondrocytes²⁸ and a liver cell line.²⁹ Viability of cells trapped by ultrasound has been measured by fluorescence microscopy, *e.g.* by the use of the viability probes calcein AM^{30,31} or acridine orange.³² The immune synapse between a natural killer cell and a target cell trapped by ultrasound was investigated with high-resolution confocal

fluorescence microscopy by Christakou *et al.*¹⁸

The position of acoustophoretically focused particles in a microchannel can be measured with optical microscopy. Manneberg *et al.*¹⁰ used confocal fluorescence microscopy to measure the 3D position of trapped beads in a sono-cage. Similar measurements were performed by Evander *et al.*³³ using a wet-etched glass chip. These experiments show that image quality and resolution do not need to be very advanced to estimate the position with sufficient accuracy.

Particle image velocimetry (PIV) has been used by many researchers for measuring either fluid velocities in acoustic streaming^{34,35} or the acoustic radiation forces acting on suspended particles in acoustofluidic devices.^{36–38} Although there are advanced and expensive PIV systems available, it is possible to use free-source-code software applied to basic microscopy video clips.

V. Conclusions

We conclude this tutorial review by summarizing a few practical recommendations when implementing optical microscopy in a lab-on-a-chip device.

Case 1: How to design a micro-device compatible with optical microscopy?

- Use the materials and thicknesses that are established as a standard^{39,40} in optical microscopy: Borosilicate glass (*e.g.* Pyrex), coverslip thickness = 170 μm and glass slide thickness = 0.8–1.0 mm. This combination makes it possible to use the device with any mode of optical microscopy, both trans- and epi-illumination based.

- The combination 170 μm and 850 μm (for the bottom and top glass layers) and 90 μm for the fluid channel is optimal for both optical microscopy and for a layered acoustic resonator.

- In general, use as shallow a micro-channel as possible, preferably a few times the size of objects studied (*e.g.* cells or beads).

- Avoid polymer materials in the optical path when performing differential interference contrast (DIC) microscopy. Polymers are also less suitable for hosting acoustic resonances.

- Optimal high-resolution imaging in the center of a fluid channel is done with a water immersion objective.

- Optimal high-resolution imaging on the bottom of a fluid channel is done with an oil immersion objective.

- Water and oil immersion mediums may cause decreased acoustophoretic performance due to acoustic transmission losses.

Case 2: How to select and operate an optical microscope for optimal performance with an existing micro-device?

- The microscope objective should not have higher magnification and numerical aperture (N.A.) than needed. 20 \times magnification and 0.3–0.7 N.A. is sufficient in many applications such as identification and characterization of individual cells. Such an objective is not very sensitive to deviations in material and thicknesses of the chip layers.

- If high-resolution microscopy is needed, an objective with a correction collar is often beneficial, in particular if the glass layer facing the objective deviates from the optimal thickness 170 μm .

- If the glass layer facing the objective is significantly thicker than 170 μm , long-working distance objectives should be used, and high-N.A. objectives (around or above 1) should be avoided. The optimal choice is to use a long-working distance objective with a correction collar and a moderate N.A. For example, there exists 40 \times /0.5 N.A. objectives which can be corrected for cover glass ranging from 0 to more than 1 mm.

- An inverted microscope is the best choice for most micro-devices. This allows for assembling all fluid connections, tubing, transducers and other bulky equipment on the upper side of the chip, while imaging from below.

- If the micro-device is non-transparent (*e.g.* a two-layer silicon-glass chip), epi-fluorescence microscopy is the most useful imaging method.

- A simple contrast-enhancing bright-field method is to insert a paper for blocking a part of the illumination light, which results in oblique illumination causing a dark-field like effect.

Acknowledgements

The authors are grateful for financial support from the Swedish Research

Council and the EU FP-7 RAPP-ID project.

References

- 1 A. Lenshof, C. Magnusson and T. Laurell, *Lab Chip*, 2012, **12**, 1210–1223.
- 2 M. Wiklund, C. Günther, R. Lemor, M. Jäger, G. Fuhr and H. M. Hertz, *Lab Chip*, 2006, **6**, 1537–1544.
- 3 C. Muñoz-Pinedo, D. R. Green and A. van der Berg, *Lab Chip*, 2005, **5**, 628–633.
- 4 M. Ochsner, M. R. Dusseiller, H. M. Grandin, S. Luna-Morris, M. Textor, V. Vogel and M. L. Smith, *Lab Chip*, 2007, **7**, 1074–1077.
- 5 B. Wang, J. Ho, J. Fei, R. L. Gonzalez Jr. and Q. Lin, *Lab Chip*, 2011, **11**, 274–281.
- 6 X. Heng, D. Erickson, L. R. Baugh, Z. Yaqoob, P. W. Sternberg, D. Psaltis and C. Yang, *Lab Chip*, 2006, **6**, 1274–1276.
- 7 X. Mao, J. R. Waldeisen, B. K. Juluri and T. Jun Huang, *Lab Chip*, 2007, **7**, 1303–1308.
- 8 G. Zheng, S. A. Lee, S. Yang and C. Yang, *Lab Chip*, 2010, **10**, 3125–3129.
- 9 A. Köhler, *Zeitschrift für wissenschaftliche Mikroskopie*, 1893, **10**, 433–440.
- 10 O. Manneberg, B. Vanherberghen, J. Svennebring, H. M. Hertz, B. Önfelt and M. Wiklund, *Appl. Phys. Lett.*, 2008, **93**, 063901.
- 11 O. Manneberg, B. Vanherberghen, B. Önfelt and M. Wiklund, *Lab Chip*, 2009, **9**, 833–837.
- 12 K. Carlsson, “*Light Microscopy*”, *KTH Physics*, Stockholm, 2007, available online at: <http://www.biox.kth.se/kjellinternet/Compendium.Light.Microscopy.pdf>.
- 13 K. Carlsson, “*Imaging Physics*”, *KTH Applied Physics*, Stockholm, 2009, available online at: <http://www.biox.kth.se/kjellinternet/Compendium.Imaging.Physics.pdf>.
- 14 R. Barnkob, I. Iranmanesh, M. Wiklund and H. Bruus, *Lab Chip*, 2012, **12**, 2337–2344.
- 15 B. Herman, “*Fluorescence Microscopy*”, Springer, USA, 1998.
- 16 M. Wiklund, *Lab Chip*, 2012, **12**, 2018–2028.
- 17 J. P. Pawley, “*Handbook of Biological Confocal Microscopy*”, 3rd Ed., Springer, USA, 2006.
- 18 A. E. Christakou, M. Ohlin, N. Kadri, T. Frisk, B. Önfelt and M. Wiklund, *Characterization of Natural Killer cells' cytotoxic heterogeneity using an array of sono-cages*, Proc. of Micro-TAS 2012, Okinawa, Japan.
- 19 H. Bruus, *Lab Chip*, 2012, **12**, 20–28.
- 20 A. Lenshof, M. Evander, T. Laurell and J. Nilsson, *Lab Chip*, 2012, **12**, 684–695.
- 21 O. Manneberg, J. Svennebring, H. M. Hertz and M. Wiklund, *J. Micromech. Microeng.*, 2008, **18**, 095025.
- 22 S. Radel, L. Gherardini, A. J. McLoughlin, O. Doblhoff-Dier and E. Benes, *Bioseparation*, 2001, **9**, 369–377.
- 23 J. F. Spengler and W. T. Coakley, *Langmuir*, 2003, **19**, 3635–3642.
- 24 M. Wiklund, J. Toivonen, M. Tirri, P. Hänninen and H. M. Hertz, *J. Appl. Phys.*, 2004, **96**, 1242–1248.
- 25 M. Wiklund and H. M. Hertz, *Lab Chip*, 2006, **6**, 1279–1292.
- 26 D. Bazou, G. A. Foster, J. R. Ralphs and W. T. Coakley, *Mol. Membr. Biol.*, 2005, **22**, 229–240.

- 27 D. Bazou, G. Davies, W. G. Jiang and W. T. Coakley, *Cell Commun. Adhes.*, 2006, **13**, 279–294.
- 28 D. Bazou, G. P. Dowthwaite, I. M. Khan, C. W. Archer, J. R. Ralphs and W. T. Coakley, *Mol. Membr. Biol.*, 2006, **23**, 195–205.
- 29 D. Bazou, W. T. Coakley, A. J. Hayes and S. K. Jackson, *Toxicol. in Vitro*, 2008, **22**, 1321–1331.
- 30 J. Hultström, O. Manneberg, K. Dopf, H. M. Hertz, H. Brismar and M. Wiklund, *Ultrasound Med. Biol.*, 2007, **33**, 145–151.
- 31 B. Vanherberghen, O. Manneberg, A. Christakou, T. Frisk, M. Ohlin, H. M. Hertz, B. Önfelt and M. Wiklund, *Lab Chip*, 2010, **10**, 2727–2732.
- 32 M. Evander, L. Johansson, T. Lilliehorn, J. Piskur, M. Lindvall, S. Johansson, M. Almqvist, T. Laurell and J. Nilsson, *Anal. Chem.*, 2007, **79**, 2984–2991.
- 33 M. Evander, A. Lenshof, T. Laurell and J. Nilsson, *Anal. Chem.*, 2008, **80**, 5178–5185.
- 34 L. A. Kuznetsova and W. T. Coakley, *J. Acoust. Soc. Am.*, 2004, **116**, 1956–1966.
- 35 M. Ohlin, A. E. Christakou, T. Frisk, B. Önfelt and M. Wiklund, *Analysis of trapping and streaming in an ultrasound-actuated multi-well microplate for single-cell studies*, Proc. of Micro-TAS 2012, Okinawa, Japan.
- 36 S. M. Hagsäter, T. Glasdam Jensen, H. Bruus and J. P. Kutter, *Lab Chip*, 2007, **7**, 1336–1344.
- 37 O. Manneberg, S. M. Hagsäter, J. Svennebring, H. M. Hertz, J. P. Kutter, H. Bruus and M. Wiklund, *Ultrasonics*, 2009, **49**, 112–119.
- 38 P. Augustsson, R. Barnkob, S. T. Wereley, H. Bruus and T. Laurell, *Lab Chip*, 2011, **11**, 4152–4164.
- 39 H. Becker, *Lab Chip*, 2010, **10**, 1894–1897.
- 40 H. van Heeren, *Lab Chip*, 2012, **12**, 1022–1025.